PERGAMON

Journal of Atmospheric and Solar-Terrestrial Physics 61 (1999) 619–628

Journal of ATMOSPHERIC AND SOLAR-TERRESTRIAL PHYSICS

Determining the drift velocity of ionospheric irregularities by analyzing three mutually orthogonal projections of the HF radio signal field vector

E.L. Afraimovich*, V.A. Kobzar, K.S. Palamartchouk

Institute of Solar-Terrestrial Physics SD RAS, PO Box 4026, Irkutsk, 664033, Russia

Received 11 June 1998; received in revised form 8 March 1999; accepted 24 March 1999

Abstract

This paper presents results of an experimental verification of our earlier suggested spectral-polarization method of measuring the interference pattern velocity by analyzing three mutually orthogonal projections of the radio signal field vector using a single receiving antenna. The measurements were made on an HF radio path about 100 km in length, with a simultaneous monitoring of the ionospheric situation using an oblique-incidence sounding chirp–ionosonde. In an effort to eliminate multipath effects, in the analysis we used nighttime intervals, for which a stable one-mode reflected radio signal was observed. It is shown that the proposed method gives the mean values of the azimuth and zenith angle which differ by no more than 2 to 5° from calculated values. Mean values of the velocity of travelling ionospheric disturbances (of order 50 m/s) and propagation directions (north-westward changing to northward by the morning hours) obtained for these time intervals are consistent with existing published data.

1. Introduction

The drift velocity of ionospheric irregularities is usually determined by measuring the velocity of the interference pattern (IP) of the ionosphere-reflected radio signal received at spaced receiving antennas (at least three antennas). Earlier we suggested a method to measure the displacement velocity of the IP by analyzing three mutually orthogonal projections of the field vector of the radio signal using a single receive antenna (Afraimovich and Palamartchouk, 1998). The first stage of analysis involves calculating complex Doppler spectra of time variations in these projections. After that, for each component of the spectra these data are used to determine the angle-of-arrival spectra. When coupled with data on Doppler shift this allows us to estimate the velocity and direction of IP displacement. In this paper which, basically is Part II of Afraimovich and Palamartchouk (1998), we gave formulae to illustrate the proposed technology, as well as results of a numerical simulation to demonstrate the possible practical implementation of the idea in the presence of additive noise and interference of different radio signal modes.

In a pioneering paper (Morgan and Evans, 1951), and in our paper (Afraimovich and Palamartchouk, 1998), this approach was considered under conditions applicable to free space. They disregarded, however,

* Corresponding author. Fax: +7-3952-462-557.
E-mail address: afra@iszf.irk.ru (E.L. Afraimovich)

1364-6826/99/$ - see front matter
PII: S1364-6826(99)00018-8

the possible effects of the mutual influence of the antennas (projections of a three-component antenna), as well as reflections of the radio wave from the underlying surface and surrounding objects. Unfortunately, the influence of these factors defies virtually all attempts to make an accurate theoretical numerical estimation. Hence, it was exceptionally important to test the performance of the method reported by Morgan and Evans (1951) and by Afraimovich and Palamartchouk (1998) in real conditions. Also, to eliminate multipath effects, we made an analysis of time intervals for which a stable one-mode reflected radio signal was observed. It should also be mentioned that we are unaware of any publications where the methods reported in Morgan and Evans (1951) and Afraimovich and Palamartchouk (1998) were tested in HF measurements.

The purpose of this study is to present the results of an experimental verification of the method from the paper of Afraimovich and Palamartchouk (1998) on a short-range HF radio path. We used angle-of-arrival and Doppler shift time dependencies to determine the velocity of a phase IP in the range of time intervals characteristic for medium-scale travelling ionospheric disturbances (TID) (periods of 30 to 60 min, and the typical size of the order of 100 to 200 km).

As is well known, TIDs are of considerable interest in ionospheric physics and as a factor limiting the accuracy of existing radio engineering systems used in navigation and radio interferometry. TIDs were treated in numerous publications (see a review on atmospheric gravity waves (AGW) and TIDs by Hocke and Schlegel, 1996). Some experimental data on TID dynamics were obtained by vertical- or weakly oblique-incidence sounding methods in the HF range using the spaced-antenna reception arrangement with a short baseline, substantially smaller than the typical size of TIDs (Afraimovich et al., 1978; Afraimovich, 1982; Jacobson and Carlos, 1989).

The correspondence between space-time characteristics in the antenna array plane obtained through vertical- or weakly oblique-incidence soundings and local characteristics of ionospheric disturbances has been discussed at length in many publications (see, for example, Afraimovich, 1982; Jacobson and Carlos, 1989) and is therefore not taken up here. The most important conclusion in the cited papers is that, as in the case of a much used model for the 'mirror phase screen' (Pfister, 1971; Afraimovich, 1982), phase disturbances of the reflected radio signal recorded in vertical- and oblique-incidence soundings are a faithful representation of the horizontal part of the corresponding local density disturbance and can be used in experimental measurements of the TID azimuth and velocity.

2. Determining the displacement velocity of the interference pattern by measuring angles of arrival and Doppler shift

Based on a relatively general example of ionospheric vertical-incidence sounding we now consider the main principles used in determining the velocity of IP displacement in terms of a simple interference model (Afraimovich, 1982) whose essential conclusions coincide with numerous existing methods of analyzing data from coherent spaced-antenna reception (see, for example, Pfister, 1971; Afraimovich et al., 1978; Afraimovich, 1982).

A complex amplitude of the radio signal at a particular point on the Earth's surface with coordinates $x = y = 0$ at time t may be represented as a discrete set of s-modes (rays):

$$\tilde{A}(x, y, t) = \sum_{s=1}^{n} r_s \exp(j(kP_s + \varphi_s(0))) \tag{1}$$

where r_s is amplitude, P_s is the phase path of the signal, $k = 2\pi/\lambda$; λ is the working frequency wavelength, $\varphi_s(0)$ is the initial phase, and n is the number of modes.

Let us consider the spatial properties of $\tilde{A}$ in the closely-spaced antenna approximation. It is also assumed that in the case of small space-time increments the distances between receiving antennas are much smaller than the typical spatial scale of a disturbance in the antenna array plane and that the time interval Δt between counts is much shorter than the disturbance time scale; hence the influence of second-order derivatives can be neglected.

In this case the phase front of the signal s-component can be considered flat and the coefficient r can be taken to be independent of the coordinates y (measured in the northward direction) and x (measured in the eastward direction), so that the signal at the spaced antennas differs only by the phase delay dependent on the coordinates of the antennas and on time t:

$$kP_s(x, y, t) = k_{x,s}x + k_{y,s}y - \omega_s t$$

$$k_{x,s} = k \sin\theta_s \sin\psi_s$$

$$k_{y,s} = k \sin\theta_s \cos\psi_s \tag{2}$$

where θ is the elevation reckoned from the zenith, ψ is the azimuth angle of arrival reckoned from the northward direction to the East, and ω is the Doppler shift. The geometry of the experiment is schematically shown in Fig. 1.

Then the velocity V_s and the propagation direction

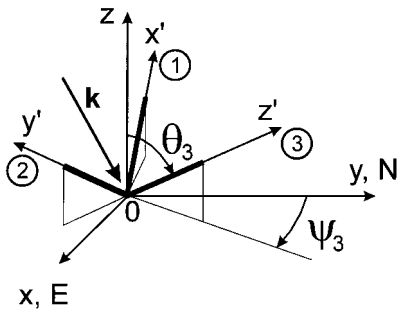

Fig. 1. Frame of reference ($x'0y'$) of the three-component antenna, and geographic coordinate system ($x0y$). In the geographic coordinate system, the axes z, y, x are pointing, respectively, to the zenith, to the North N, and to the East E. ψ'; θ'; ψ, and θ are the azimuths and zenith angles of the wave vector $\mathbf{k}$ in the above coordinate systems, and ψ_j and θ_j are the corresponding angular coordinates of j-projections of the three-component antenna; $j = 1, 2, 3$. The figure also shows the angular coordinates ψ_3 and θ_3, corresponding to the third projection of the three-component antenna.

α_s of the phase front of the radio signal s-component in the plane ($x0y$) are determined by the values of the angles of arrival and Doppler frequency (Afraimovich, 1982):

$$V(\omega_s) = \omega_s/2\sqrt{k_{x,s}^2 + k_{y,s}^2}$$

$$\alpha(\omega_s) = \arctan(k_{x,s}/k_{y,s}) \tag{3}$$

Well-known methods of spectral analysis of the complex amplitude are used to resolve individual spectral components and determine velocity parameters using (3).

Measurements of Doppler frequencies using state-of-the-art highly stabilized oscillators at the transmitting and receiving ends of the radio path present no special problems. Thus the solution of the formulated problem is dictated by the accuracy with which it is possible to determine the radio wave's angles of arrival using a three-component antenna.

3. Determining angle of arrival from three mutually orthogonal components of the field vector

It was shown in an earlier paper (Morgan and Evans, 1951) that in free space the complex amplitudes of three mutually-orthogonal projections of the one-mode regular signal field determine parameters of the polarization ellipse and the sense of rotation of the polarization vector, as well as the angles of arrival ψ and θ (position of the wave front). The above parameters compose a description of the full vector of a plane radio wave and are related to the complex amplitudes $\tilde{A}_x$, $\tilde{A}_y$, $\tilde{A}_z$ of field projections by a system of transcendental equations (the axis z is pointing towards the zenith):

$$\tilde{A}_x = A_x \exp(j\varphi_x)$$

$$\tilde{A}_y = A_y \exp(j\varphi_y)$$

$$\tilde{A}_z = A_z \exp(j\varphi_z) \tag{4}$$

Morgan and Evans (1951) developed a method to analyze and synthesize a three-component field for the one-mode signal. An extension of the method to the case of a multimode radio signal was suggested in Afraimovich and Palamartchouk (1998), implying a spectral-polarization technique for analyzing the full vector of the radio wave field, based on complex Doppler mode filtering. The essence of the method is that in all algorithms for computing parameters of the field's full vector using systems of equations for mutually orthogonal projections of the field, in lieu of complex amplitudes of projections, complex amplitudes of complex Doppler spectrum components of these projections are used, that is, amplitude $S_x(\omega)$, $S_y(\omega)$, $S_z(\omega)$ and phase $\Phi_x(\omega)$, $\Phi_y(\omega)$, $\Phi_z(\omega)$ spectra, where ω is the angular frequency. These spectra are calculated for x-, y- and z-complex amplitudes of the output signal from the corresponding mutually orthogonal antennas using Fast Fourier Transform (FFT) algorithms and suitable time and spectral windows.

Without going into a detailed description of the algorithms (Afraimovich and Palamartchouk, 1998), we write here formulae defining angles of arrival of a plane wave in free space:

$$\cot\ \psi(\omega) = \frac{s_x(\omega)\ \sin\ (\Delta_{xz}(\omega))}{s_y(\omega)\ \sin\ (\Delta_{zy}(\omega))}$$

$$\tan^2(\omega) = \frac{S_x^2(\omega)S_z^2(\omega)\ \sin^2(\Delta_{xz}(\omega)) + S_z^2(\omega)S_y^2(\omega)\ \sin^2(\Delta_{zy}(\omega))}{S_y^2(\omega)S_x^2(\omega)\ \sin^2(\Delta_{yx}(\omega))} \tag{5}$$

where $\Delta_{yx}(\omega) = \varphi_y(\omega) - \varphi_x(\omega)$, $\Delta_{zy}(\omega;) = \varphi_z(\omega) - \varphi_y(\omega)$, $\Delta_{xz}(\omega) = \varphi_x(\omega) = -\varphi_z(\omega)$. Not only does complex Doppler filtering make it possible to separate the interfering modes, but it also enhances the noise immunity of measurements and hence the stability of the solution of Eqs. (5).

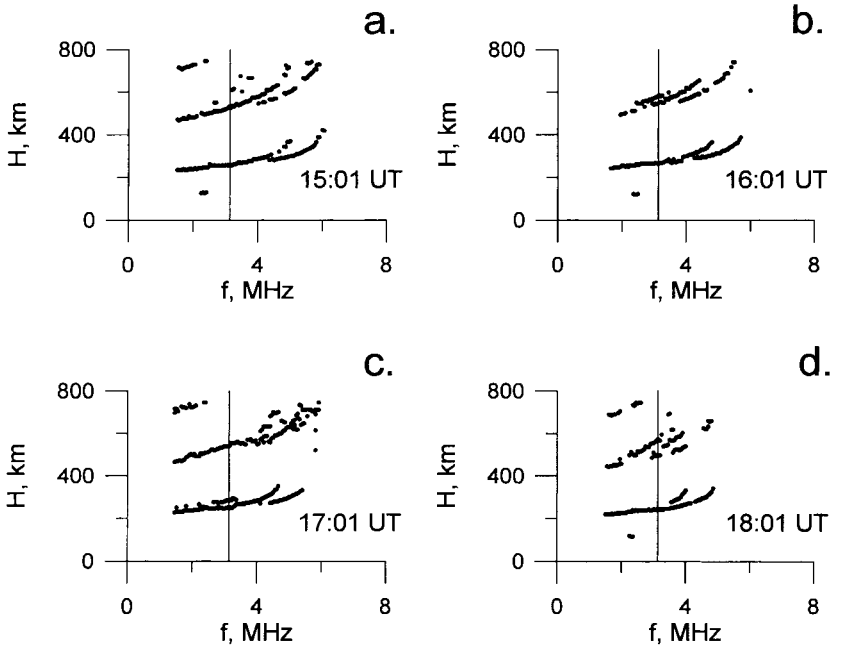

Fig. 2. Chirp–ionosonde ionograms taken on 25 June 1997 from 15:01 to 18:01 UT [(a) 15:01 UT; (b) 16:01 UT; (c) 17:01 UT; (d) 18:01 UT]. The vertical bar shows the value of the sounding frequency of 3.13 MHz.

4. General description of the experiment and data treatment

For an experimental verification of the method, a special-purpose facility was designed for measuring and recording the complex amplitudes of three mutually orthogonal projections of the full vector of the radio wave field. The measurements were made on a path 113 km in length, with the geographical azimuth $\psi_0 = 64^\circ$, by sounding with a continuous HF radio signal at the sounding frequency $f = 3.13$ MHz.

The particular working frequency was determined based on average data of oblique-incidence ionospheric soundings to correspond to the middle point of the path for the selected time interval. These measurements were carried out every hour with the chirp–ionosonde described in Brynko et al. (1988). Most data were obtained for the nighttime when reflection was from the ionospheric F2-region. To illustrate experimental results, we selected a typical time interval, from 15:00 to 21:00 UT on 25 June 1997 (from 22:00 LT on 25 June to 04:00 LT on 26 June).

Fig. 2 presents the frequency dependencies of the effective reflection height $H(f)$ of the HF radio signal (ionograms) measured on 25 June 1997 from 15:00 to 18:00 UT with the chirp–ionosonde [(a) 15:01 UT; (b) 16:01 UT; (c) 17:01 UT; (d) 18:01 UT]. The vertical bar shows the value of the sounding frequency. It is evident from the figure that typically the ordinary component of the reflected signal was recorded at the selected sounding frequency, and corresponding values of the effective height were determined for the selected time interval in the range from 230 to 270 km.

It should be noted that in Fig. 2 the information about the frequency dependence $H(f)$ of the single and double signals is plotted without regard for the relative amplitude of these signals; the double signals in these measurements are an order of magnitude weaker. Furthermore, despite the relative proximity of the transmitter, we were also able to neglect the influence of the ground wave because its additional attenuation was caused by the fact that between the reception facility and the transmitter there was a mountain range. In the first approximation, we can therefore conceive of the measurements as being made for the one-ray (one-mode) radio signal.

The recording system included (Fig. 3):

- antenna-feeder system (AFS);
- radio-engineering system (RES);
- hardware-computing system (HCS);
- exact time and frequency system (ETFS);
- personal computer IBM AT (PC).

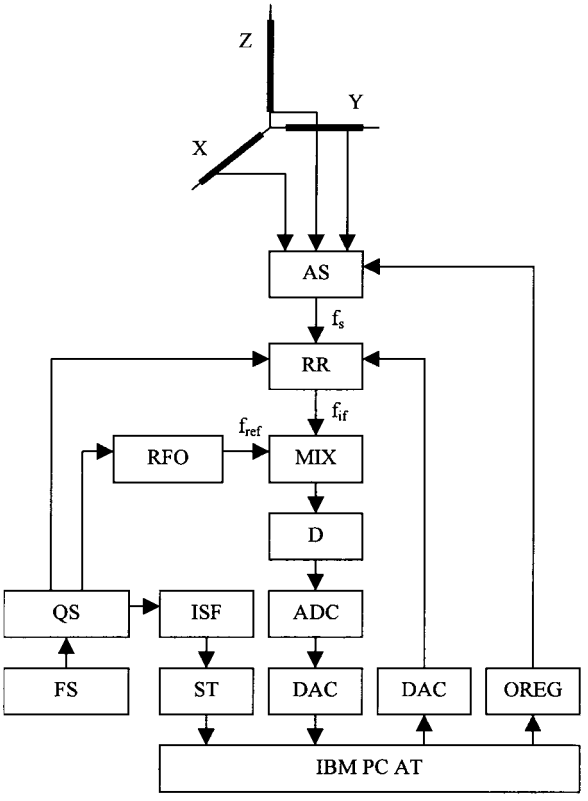

Fig. 3. Block-diagram of the measuring facility (explanations are given in the text).

Measurements at the facility with the necessary frequency stability were secured by the ETFS consisting of the time and frequency standard FS, the quartz synchronometer QS, and the reference frequency oscillator f_{ref} RFO. The accuracy of measurements was determined by the FS frequency instability and was of order of 10^{-11}.

The AFS, consisting of three mutually orthogonal magnetic antennas (X, Y, Z) and the antenna switch (AS), converted the electromagnetic wave energy to electrical signals proportional to the projections of the full vector of the wave field. Phase calibration of the AFS was done by feeding the calibration signal simultaneously to all cable inputs of the reception system (instead of the signal from the antennas); phase corrections, calculated for each of the working frequencies of the range, were entered into the PC and were taken into account in the processing.

We used special-purpose direction-finder cavity magnetic antennas to receive signals only from the upper hemisphere by screening secondary signals reflected from the Earth's surface. Magnetic dipoles were aligned along the axes of the antenna frame of reference in such a manner as shown in Fig. 1 by heavy lines. The figure also shows the angular coordinates ψ_3 and θ_3, corresponding to the third projection of the three-component antenna.

A calculation of the expected zenith angle θ_0 for this path using the data from the chirp–ionosonde based on Martin's theorem from the familiar relationships (Davies, 1969) showed that $\theta_0 = 10$ to 12°. Therefore, the best choice from the point of view of the attenuation of interference effects caused by reflection from the Earth's surface and from surrounding objects was such an orientation of the antennas' coordinate system where the symmetry axis of the three-component antenna was pointing to the zenith. Results presented below were obtained for the values of $\theta_j = 55^\circ$; $\psi_1 = 240^\circ$, and $\psi_2 = 120^\circ$, and $\psi_3 = 0^\circ$.

The RES, consisting of the radio receiver (RR) and the mixer (MIX), provided the main amplification, filtering and double conversion of the received signal frequency and the mixing of the signal of the second intermediate frequency f_{if} of the radio receiver with the signal of the reference frequency f_{ref}. The RR was tuned to the frequency f, above or below the signal frequency of the radio station f_s, so that the detuning frequency Δf was larger than the maximum expected spectrum width of the carrier (1.5 to 2 Hz) (Afraimovich, 1982). The beat signal at the frequency Δf from the detector output (D) and the direct-current amplifier (DCA), which is the signal of the last intermediate frequency, was fed to the analogue-digital converter (ADC) input. The PC was used in recording this signal, controlling the antenna switch (AS) by means of the output register (OREG), and in controlling the RR amplification using the digital-analogue converter (DAC). To synchronize the process of recording and controlling the signals from the synchronometer QS, the interrupt signal former (ISF) and the synchronizer-timer (ST) was employed.

At the first stage of data processing, the series obtained (4) were fast-Fourier transformed with the length of a series of 512 counts, which corresponded to the integration time of about 32 s and a frequency resolution of 0.03 Hz. The particular length of the series was determined by the required time resolution of the secondary data processing in order to determine the TID propagation velocity (see below). Of course, this led to a decrease in frequency resolution of the various modes of the reflected signal. However, as has been pointed out above, in the analysis we used time intervals predominantly with a one-ray signal, so that this impairment did not affect our final results.

The series of amplitude $S_x(\omega)$, $S_y(\omega)$, $S_z(\omega)$ and phase $\Phi_x(\omega)$, $\Phi_y(\omega)$, $\Phi_z(\omega)$ spectra in the design of the proposed algorithm are the results of data treatment; further analysis of the signal, however, was car-

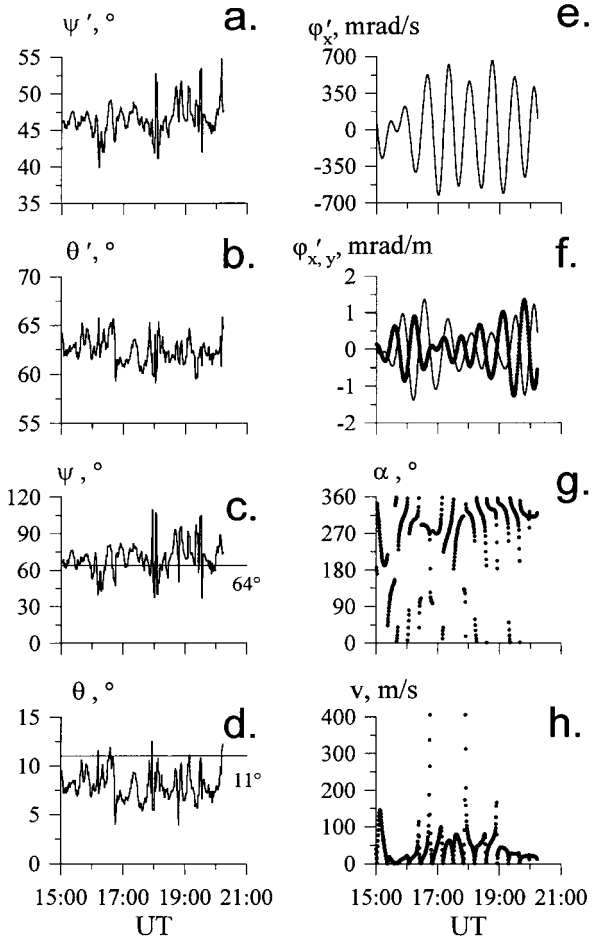

Fig. 4. Time dependencies of the azimuth $\psi'(t)$ and zenith angle $\theta'(t)$ in the antenna's frame of reference (a, b) and $\psi(t)$ and $\theta(t)$ in the geographic coordinate system (c, d) measured on 25 June 1997 from 15:00 to 21:00 UT and smoothed with a 5-min time window. Variations in space-time characteristics of the phase derivatives, corresponding to these data and filtered in the range 30 to 60 min, and also variations in the azimuth and velocity modulus of IP displacement [(e) $\phi'_t(t)$; (f) $\phi'_x(t)$, line; $\phi'_y(t)$, dots; (g) $\alpha(t)$; (h) $v(t)$]. The horizontal bar on panels (c, d) shows values of the actual azimuth to the transmitter (64°) and of the zenith angle calculated based on ionospheric sounding data from the chirp–ionosonde (11°).

ried out in the complex Fourier-domain. Depending on the tackled problem, different algorithms for secondary processing of these series may be suggested. For our chosen variant with a one-ray signal, it was best simply to average the amplitude and the phase difference for those spectral components whose amplitude was higher than the specified relative threshold ϵ (in our case $\epsilon = 0.9$), followed by the determination of the angles of arrival using formulae (5).

5. Measuring the angles of arrival using a three-component antenna

At the left of Fig. 4, we present time dependencies of the azimuth $\psi'(t)$ and zenith angle $\theta'(t)$ in the antenna's frame of reference (a, b) and $\psi(t)$ and $\theta(t)$ in the geographical coordinate system (c, d) which were measured on 25 June 1997 from 15:00 to 21:00 UT and smoothed with the 5-min time window. Horizontal bars show the true value of the azimuth $\psi_0 = 64^\circ$ and the calculated value of the zenith angle $\theta_0 = 11^\circ$.

Angles of arrival are converted from the antenna's frame of reference to the geographical coordinate system, described in Section 1, in the following manner. Let the antenna array be characterized by three pairs of numbers (with consideration for the designations in Fig. 1): (ψ_1, θ_1), (ψ_2, θ_2), (ψ_3, θ_3), where θ is the angle between the zenith and the antenna direction, and ψ is the azimuthal angle of the antenna projected onto the geographic horizontal plane. Such a representation of the antenna array geometry is redundant because the angles between the antennas remain unchanged and are $\pi/2$, but it is convenient for subsequent transformations. Let also the absolute values of the antennas' direction vectors be 1.

The geographical coordinates of the direction vector $\mathbf{a}_j$ of the antenna j then take the form:

$$a_{x,j} = \sin\theta_j \sin\psi_j$$

$$a_{y,j} = \sin\theta_j \cos\psi_j$$

$$a_{z,j} = \cos\theta_j \qquad (6)$$

In an analogous way, we characterize the direction to the 'source' of the received radio wave, which is equivalent to the direction of the vector $-\mathbf{k}$:

$$-k_x = \sin\theta \sin\psi$$

$$-k_y = \sin\theta \cos\psi$$

$$-k_z = \cos\theta \qquad (7)$$

The projections of the vector $-\mathbf{k}$ onto the antennas' direction vectors $\mathbf{a}_j$ are then equal to their scalar products:

$$-\mathbf{k}\mathbf{a}_1 = -(k_x, k_y, k_z)(a_{x,1}, a_{y,1}, a_{z,1}) = \sin\theta' \sin\psi'$$

$$-\mathbf{k}\mathbf{a}_2 = -(k_x, k_y, k_z)(a_{x,2}, a_{y,2}, a_{z,2}) = \sin\theta' \cos\psi'$$

$$-\mathbf{k}\mathbf{a}_3 = -(k_x, k_y, k_z)(a_{x,3}, a_{y,3}, a_{z,3}) = \cos\psi' \qquad (8)$$

where θ' and ψ' are the direction angles of the vector $-\mathbf{k}$ in the antenna's frame of reference.

On solving this system of equations, we obtain expressions for the angles of arrival of the radio wave in the geographic coordinate system:

$$\tan\ \psi = k_x/k_y$$

$$\tan\ \theta = \sqrt{k_x^2 + k_y^2}/k_z \tag{9}$$

These results are correct for the magnetic part of the electromagnetic field of the radio wave.

For the selected time interval presented in Fig. 4, the mean values and the root-mean-square deviation (r.m.s.) of the azimuth $\psi'(t)$ in the antenna's frame of reference were, respectively, 46.6 and 2.7° (panel a), and those of the zenith angle $\theta'(t)$ were 62.3 and 2.3° (panel b). Upon conversion to the geographic coordinate system by formulas (6)–(9) the corresponding values for the azimuth were 70 and 14° (panel c), and those for the zenith angle were 8.2 and 2.7° (panel d).

As can be made certain, the estimated mean value of the zenith angle is less than the calculated value by no more than by 2 to 3°, and that the azimuth is larger than the calculated value by 6°. Considering the fact that the accuracy of installation of the platform with a three-component antenna with respect to the geographic coordinate system was only to a few degrees, such a result may be regarded as quite a convincing validation of the proposed method for determining the angles of arrival.

In regard to angle-of-arrival variations whose amplitude can be inferred from corresponding r.m.s. values, they correlate quite well with published data obtained on short-range HF paths using conventional methods of angle-of-arrival measurement (Reynolds and Morgan, 1975; Jones and Reynolds, 1975; Lyon, 1979; Afraimovich, 1982; Afraimovich et al., 1985). It should be noted that oscillations with typical periods between 10 min and 1 h are especially pronounced in angle-of-arrival variations. It is commonly believed that these oscillations are caused by medium-scale travelling ionospheric disturbances, forming the basis for appropriate methods of monitoring these disturbances in spaced-antenna reception with a small baseline (see, for example, Reynolds and Morgan 1975; Jones and Reynolds, 1975; Lyon 1979; Afraimovich, 1982; Afraimovich et al., 1985; Jacobson and Carlos, 1989). In this paper, we have also drawn on angle-of-arrival measurements in conjunction with Doppler shift measurements to determine the horizontal velocity component of TIDs.

6. Determining the velocity of medium-scale travelling ionospheric disturbances

We determine the travel velocity and direction of the phase IP (phase front) in the horizontal plane in terms of some model for this pattern, an adequate choice of which is of critical importance. Space-time variations in the radio signal phase $\Delta\phi(x, y, t)$ at each given instant of time t may be represented in the simplest form as a phase front propagating without a change in the form (no dispersion):

$$\Delta\phi(x, y, t) = F(t - x/v_x - y/v_y) \tag{10}$$

where v_x and v_y are the velocity of the phase front travelling along the axes x and y, respectively.

It should be noted, however, that in real situations an ideal model (10) is not realized in a pure form. This is because acoustic-gravity waves that cause TIDs propagate in the atmosphere in the form of a dispersed wave packet with a finite value of the angular spectrum width. But to a first approximation, for short averaging times comparable with the period of filtered variations in the signal phase, the phase IP may be thought of as travelling without a substantial change in its form.

In this paper, we employ a statistical angle-of-arrival and Doppler method (SADM) for determining characteristics of the TID dynamics based on measuring the spatial derivatives $\phi'_x(t)$ and $\phi'_y(t)$ proportional to the values of direction angles of arrival of sounding radio signals, and the time derivative $\phi'_t(t)$ proportional to the frequency Doppler shift of these signals, which was described in detail in some publications (Afraimovich et al., 1997; Afraimovich, 1998):

$$\phi'_t(t) = \Omega(t)/2$$

$$\phi'_x(t) = k\ \sin\ \theta(t)\ \sin\ \psi(t)$$

$$\phi'_y(t) = k\ \sin\ \theta(t)\ \cos\ \psi(t) \tag{11}$$

The factor 2 is included here, which is valid for the variant of vertical- or weakly oblique-incidence sounding (Afraimovich, 1982). It should also be noted that in the case of oblique-incidence soundings corresponding series of phase derivatives must be centred on their mean values in order to eliminate the influence of the orientation of the radio sounding path. In the present case we took this factor into account in band filtering of the initial series in the selected range of 30 to 60 min periods (see below).

SADM makes it possible to establish the azimuth $\alpha(t)$ of the IP wave vector (normal to the phase front) in the range 0 to 360°, as well as to determine the velocity modulus $v(t)$ at each instant of time by formulae:

$$W_y(t) = \phi'_y(t)/\phi'_t(t) = \mid W \mid \cos\ \alpha$$

$$W_x(t) = \phi'_x(t)/\phi'_t(t) = \mid W \mid \sin\ \alpha$$

$$v(t) = \mid W \mid^{-1} = (W_x^2(t) + W_y^2(t))^{-1/2} \quad (12)$$

Time dependencies of the velocity $v(t)$ and azimuth $\alpha(t)$ obtained from (12) can then be used to construct, for the selected time interval, the distribution functions of the azimuth $P(\alpha)$ and velocity $P(v)$. In the case of the ideal IP (10) the transformations (12) give a time-constant value of the azimuth and velocity, while the distribution functions $P(\alpha)$ and $P(v)$ have well-defined maxima at these values. In real situations, these distributions are broadened, which is due primarily to dispersive changes in the spectrum of the TIDs as they propagate in the atmosphere.

By analyzing the time dependence $\alpha(t)$ and the distribution $P(\alpha)$, it is possible to estimate the azimuth of the predominant propagation of TIDs. If such a direction does exist, then the pattern may be thought of as travelling without a change in the form, and the mean velocity of its displacement can be determined either from the velocity distribution $P(v)$ or by a direct averaging of instantaneous values of $v(t)$. One can select different existence criteria for a distinct propagation direction; however, it would be most natural to estimate the azimuth r.m.s. α. If r.m.s. exceeds 90°, then there is no point in arguing for a directional displacement of the interference pattern. If, however, r.m.s. α is markedly less than 90°, one can argue that the pattern travels mainly in the direction of the mean value of the azimuth. For the purposes of this study, the values of phase derivatives were determined from angle-of-arrival and Doppler measurements by formulas (11) and were filtered in the range of 30 to 60 min periods characteristic for medium-scale TIDs.

It is possible to determine the horizontal velocity component of TIDs using the algorithm of (12) both from angle-of-arrival measurements in the geographic coordinate system, as well as in the antenna's frame of reference, followed by a conversion to the geographic coordinate system using formulas (6)–(9), only of the mean values of the azimuth α and velocity v for the selected time interval. The second variant proved to be more advantageous as it permitted us to minimize the influence of errors arising in the conversion to the geographical coordinate system, by (6)–(9), of each of the instantaneous values of angles of arrival determined in the antenna's frame of reference.

Fig. 4 presents time dependencies of space-time characteristics of phase derivatives in the antenna's frame of reference, and of the values of $\alpha(t)$ and $v(t)$, inferred from formulae (12) and (6)–(9), which correspond to variations in the zenith angle $\theta'(t)$ and azimuth $\psi'(t)$ given in this figure (left) in the antenna's frame of reference [(e) $\phi'_t(t)$; (f) $\phi'_x(t)$ line; $\phi'_y(t)$, dots; (g) $\alpha(t)$; (h) $v(t)$].

For the selected time interval shown in Fig. 4(g, h), the mean values and r.m.s. of the azimuth $\alpha(t)$ of the phase IP travelling in the plane ($x0y$) of the geographic coordinate system were, respectively, 326 and 36°, and those of the velocity $v(t)$ 43 and 44 m/s. A relatively large spread in displacement velocities and directions on Fig. 4(g, h) is caused primarily by the discrepancy between the experimentally observed IP and the ideal model of the phase front that is displaced without changing its shape (formula 10).

Since r.m.s. of the azimuth (36°) are markedly less than 90°, based on the above reasoning we can argue that in the course of the selected nighttime interval the interference pattern was mainly displaced with the average velocity of about 43 m/s in the north-western direction and changed to northward by the morning hours. This result correlates quite well with existing models for the generation and propagation of TIDs (see a review by Hocke and Schlegel, 1996), as well as with currently available (but, unfortunately, few in number) published data of nighttime measurements obtained through vertical- or oblique-incidence ionospheric soundings using spaced-antenna reception with a long baseline comparable with the TID size (Munro, 1958; Morton and Essex, 1978; Bowman, 1981; Drobzhev et al., 1988; Hocke and Schlegel, 1996).

7. Conclusions

The results presented in this work suggest the following conclusions:

1. The proposed method gives stable mean values of the azimuth and zenith angle of arrival which differ from calculated values by no more than 2 to 5°.
2. The mean velocities of travelling ionospheric disturbances (of about 50 m/s) and propagation directions (north-westward changing to northward by the morning hours), obtained for these time intervals, are consistent with existing published data.
3. The use of the proposed method can improve the spatial resolution in remote sensing from such mobile platforms as ships at sea and satellites (also in the case of topside soundings), as well as in the configuration of classical spaced-antenna reception but with the use of three-component receive antennas. This last variant combines two independent methods for measuring angles of arrival, which affords a substantial improvement to the reliability of the measurements and provides new information about, for example, the curvature of the interference pattern front.

Our intention in this paper is to demonstrate experimentally the fundamental possibility of measuring angles of arrival and the displacement velocity of the phase IP without invoking the space-diversity reception. In this case we were able to assess the validity of angle-of-arrival measurements only on the basis of the data on the radio path geometry. As far as the measurements of the phase IP displacement velocity are concerned, we confined ourselves solely to the comparison with published data. In accordance with the chief objective of our work, we restricted our analysis to the one-mode signal only, because analyzing the applicability of the method under multi-mode propagation conditions is a separate independent problem.

Unfortunately, for technical reasons and due to experimental conditions, the amount of experimental material suitable for processing was quite small, so it was not possible for us to obtain the necessary data for evaluating the performance of the technique under different geophysical conditions, as well as under multi-mode propagation conditions. We understand that such a comparison is insufficient for an adequate assessment of the attainable accuracy and reliability of the results.

Because of our limited resources, we were also unable to carry out experiments aimed at a 'direct' comparison of related experiments using our suggested method and existing classic facilities (HF direction finders, Dynasondes, etc.). At some future date it will be necessary to conduct a series of comprehensive experiments using, among other things, movable platforms.

Acknowledgements

We are indebted to V. E. Nosov and V. I. Kurkin for providing us with chirp-sounding data spanning the period of our measurements. Thanks are also due to V. V. Chernukhov and O. N. Boitman for help in carrying out the experiment. The authors thank V. G. Mikhalkovsky for his assistance in preparing the English version of the manuscript, and the two referees for their great contribution. This work was done with support from the Russian Foundation for Basic Research—Grant Nos. 96-05-64162 and 97-02-96060.

References

Afraimovich, E.L., 1982. Interference Methods of Ionospheric Radio Sounding. Nauka, Moscow.

Afraimovich, E.L., 1988. Statistical method for determining characteristics of the dynamics of the radio interference pattern. In: Wilkinson, P.J. (Ed.), Proceedings of the XXVth URSI General Assembly, Lille '96, Rep. UAG-105. World Data Center A for Solar-Terrestrial Physics, National Geophysical Data Center, Boulder, CO, USA, pp. 103–108.

Afraimovich, E.L., Palamartchouk, K.S., 1998. Determining the velocity of the interference pattern by analyzing three mutually orthogonal projections of the radio signal field vector. Part I. Numerical simulation. Journal of Atmospheric and Solar-Terrestrial Physics 60, 115–120.

Afraimovich, E.L., Boitman, O.N., Zhovty, E.I., Kalikhman, A.D., Pirog, T.G., 1997. Dynamics and anisotropy of travelling ionospheric disturbances as deduced from transionospheric sounding data. Geomagnetizm i aeronomya 37, 86–94.

Afraimovich, E.L., Vugmeister, B.O., Zacharov, V.N., Kalikhman, A.D., Korolev, V.A., 1978. Experimental investigation of fluctuations of radio signal Doppler frequencies and angles of arrival by vertical-incidence sounding of the ionospheric F2 layer. Izvestia Vuzov Radio Physics 21, 338–347.

Afraimovich, E.L., Ashkaliev, Ya. F., Belyaev, M.A., Vyborov, V.I., Lysak, A.V., Udodov, M. Yu., 1985. Variation of HF radio signal arrival angles and medium-scale travelling ionospheric disturbances. Issledovaniya po geomagnetizmu, aeronomii i fizike Solntsa 73, 96–104.

Bowman, G.G., 1981. The nature of ionospheric spread-F irregularities in mid-latitude regions. Journal of Atmospheric and Terrestrial Physics 43, 65–79.

Brynko, I.G., Galkin, I.A., Grozov, V.P., Dvinskikh, N.I., Matyushonok, S.M., Nosov, V.E., 1988. An automatically controlled data gathering and processing system using an FMCW ionosonde. Advances in Space Research 8 (4), (4)121–(4)124.

Davies, K., 1969. Ionospheric Radio Waves. Blaisdell, Waltham, MA.

Drobzhev, V.I., Kaliyev, M.Z., Krasnikov, I.M., Litvinov, Y.G., Chakenov, B.D., Yakovets, A.F., 1988. Phase velocities of medium scale travelling ionospheric disturbances. Geomagnetizm i aeronomya 28, 308–311.

Hocke, K., Schlegel, K., 1996. A review of atmospheric gravity waves and travelling ionospheric disturbances: 1982–1995. Annales Geophysicae 14, 917–940.

Jacobson, A.R., Carlos, R.C., 1989. Coherent-array HF Doppler sounding of travelling ionospheric disturbances. 1. Basic technique. Journal of Atmospheric and Terrestrial Physics 51, 257–309.

Jones, T.B., Reynolds, J.S.B., 1975. Ionospheric perturbations and their effect on the accuracy of h.f. direction finders. Radio and Electronic Engineering 45, 63–72.

Lyon, G.F., 1979. The corrugated reflector model for one-hop oblique propagation. Journal of Atmospheric and Terrestrial Physics 41, 5–9.

Munro, G.H., 1958. Traveling disturbances in the F-region. Australian Journal of Physics 11, 91–112.

Morton, F.W., Essex, E.A., 1978. Gravity wave observations at a southern hemisphere mid-latitude station using the total electron content technique. Journal of Atmospheric and Terrestrial Physics 40, 1113–1122.

Morgan, M., Evans, W., 1951. Synthesis and analysis of elliptic polarization loci in terms of space-quadrature sinusoidal components. Proceedings of IRE 39, 552–556.

Pfister, W., 1971. The wave-like nature of inhomogeneities in the E-region. Journal of Atmospheric and Terrestrial Physics 33, 999–1025.

Reynolds, J.S.B., Morgan, A.D., 1975. The effect of frequency separation on the correlation of bearing errors measured on ionospherically propagated HF signal from colocated transmitters. Journal of Atmospheric and Terrestrial Physics 37, 545–551.